

See discussions, stats, and author profiles for this publication at: <https://www.researchgate.net/publication/315593116>

Physical and Mechanical Properties of Fungal Mycelium-Based Biofoam

Article in *Journal of Materials in Civil Engineering* · March 2017

DOI: 10.1061/(ASCE)MT.1943-5533.0001866

CITATIONS

119

READS

11,306

5 authors, including:



Feng Zhang

Harbin Institute of Technology

81 PUBLICATIONS 907 CITATIONS

[SEE PROFILE](#)



Benjamin Still

University of Alaska Anchorage

14 PUBLICATIONS 316 CITATIONS

[SEE PROFILE](#)



Philippe Amstislavski

University of Alaska Anchorage

10 PUBLICATIONS 286 CITATIONS

[SEE PROFILE](#)

Some of the authors of this publication are also working on these related projects:



Biomaterials research [View project](#)



Landscape epidemiology [View project](#)

Physical and Mechanical Properties of Fungal Mycelium-Based Biofoam

Zhaohui (Joey) Yang, M.ASCE¹; Feng Zhang²; Benjamin Still, S.M.ASCE³; Maria White⁴; and Philippe Amstislavski⁵

Abstract: This paper presents an innovative fungal mycelium-based biofoam. Three different mixing protocols with various substrate materials, including wood pulp, millet grain, wheat bran, a natural fiber, and calcium sulfate, and two packing conditions were tested to produce samples for physical, thermal, and mechanical property characterization. Dry density, thermal conductivity, elastic moduli, Poisson's ratio, and compressive strength were obtained. It was found that densely packed samples following Mixing Protocol II have the highest dry density, elastic moduli, compressive strength, and comparable thermal conductivity, and have met or exceeded like characteristics of the conventional polymeric thermal foams except dry density. The results demonstrate that this biofoam offers great potential for application as an alternative insulation material for building and infrastructure construction, particularly in cold regions, or as light-weight backfill material for geoenvironmental applications. DOI: [10.1061/\(ASCE\)MT.1943-5533.0001866](https://doi.org/10.1061/(ASCE)MT.1943-5533.0001866). © 2017 American Society of Civil Engineers.

Author keywords: Fungal mycelium-based biofoam; Thermal conductivity; Elastic moduli; Compressive strength.

Introduction

Polymeric foams, such as polystyrene and polyurethane, are commonly used for thermal insulation and lightweight fill in infrastructure and housing construction. These hydrocarbon-based materials are lightweight, hydrophobic, and resistant to photolysis. They are not subject to decomposition or decay (Eben and Gavin 2011) and create problems with respect to recycling, reuse, and landfill operation. More importantly, these polymeric foams are nonrenewable and their production and use involve complex manufacturing processes, substantial energy inputs, and associated waste streams (Bandyopadhyay and Basak 2007). Polymeric foams have been shown to leach out or off-gas several toxins that bio-accumulate in fish and wildlife, presenting a well-documented environmental and public health problem (Padula et al. 2014; Hofer 2008). A renewable alternative to today's conventional thermal insulation and lightweight fill materials would substantially reduce the environmental and public health burden of construction and promote sustainable infrastructure development.

Biocomposites based on natural fibers, environmentally-friendly composites of various biopolymers, typically reinforced with natural fibers, provide promising renewable and biodegradable alternatives to petroleum-based polymeric materials (Dicker et al. 2014; Gurunathan et al. 2015). Biomass products from agro-resources, including polysaccharides and proteins, are one of many types of environmentally biodegradable polymers. Polysaccharides are the most widespread polymers in nature, playing essential roles to sustain living organisms, and are commonly known as starch, proteins, cellulose, chitin, and so on. Novel biocomposites based on these natural materials form one of the emerging areas in polymer science. For instance, Morreale et al. (2008) investigated the effects of adding wood fibers on the physical properties of a corn-starch-based biodegradable polymer. Moriana et al. (2011) synthesized a starch-based biocomposite by adding natural fibers and characterized its thermomechanical properties. Paul et al. (2015) synthesized a novel biocomposite formed by banana fibers infused with resin made from banana sap. They characterized the mechanical, thermal, and morphological properties and found the composite was suitable for general nonfunctional components.

This paper focuses on a fungal mycelium-based biocomposite that is grown rather than manufactured or synthesized. Mycelium, the vegetative part of fungus, is a hollow structure consisting of a mass of branching, hollow tubular, chitinous hyphae that provide a fast-growing, safe, and inert material as the binding matrix for a new generation of natural foams, or biofoams (Travaglini et al. 2014). As the mycelium grows, a network of branching hyphae, primarily composed of chitin, binds together the nutritive substrate consisting of biomass and creates a vast three-dimensional matrix. Biofoams offer several additional advantages over polymeric foams, including low cost of production, fast renewability, and carbon capture and storage, and can serve as replacements for the petroleum-based polymeric materials for applications in insulation, lightweight fill, packaging, noise control, and sandwich panels (Travaglini et al. 2014). Several studies on this front have revealed the unique mechanical properties and promising potential of biofoams in engineering applications. Arifin and Yusuf (2013) investigated the impact of mixing a ratio of rice husks and wheat grain on the physical properties, microstructure, and porosity of a

¹Professor, College of Engineering, Univ. of Alaska Anchorage, 3211 Providence Dr., Anchorage, AK 99508. E-mail: zyang2@uaa.alaska.edu

²Assistant Professor, School of Transportation Science and Engineering, Harbin Institute of Technology, 73 Huanghe Rd., Harbin 150090, China; Postdoctoral Researcher, College of Engineering, Univ. of Alaska Anchorage, 3211 Providence Dr., Anchorage, AK 99508 (corresponding author). E-mail: zhangf@hit.edu.cn

³Ph.D. Student, College of Engineering, Univ. of Alaska Anchorage, 3211 Providence Dr., Anchorage, AK 99508. E-mail: bastill@alaska.edu

⁴Student, Dept. of Health Sciences, Univ. of Alaska Anchorage, 3211 Providence Dr., Anchorage, AK 99508. E-mail: mdwhite2@alaska.edu

⁵Associate Professor, Dept. of Chemistry, Univ. of Alaska Anchorage, 3211 Providence Dr., Anchorage, AK 99508. E-mail: pamstislavski@alaska.edu

Note. This manuscript was submitted on June 1, 2016; approved on October 26, 2016; published online on March 23, 2017. Discussion period open until August 23, 2017; separate discussions must be submitted for individual papers. This paper is part of the *Journal of Materials in Civil Engineering*, © ASCE, ISSN 0899-1561.

mycelium biofoam. Holt et al. (2012) investigated the manufacturing of biodegradable molded packaging materials based on fungal mycelium and cotton plant materials and found these materials met or exceeded like characteristics of extruded polystyrene foam. Pelletier et al. (2013) evaluated the acoustic performance of a mycelium biofoam based on agricultural by-product substrates, and results suggested an optimal performance in automotive road noise control. Travaglini et al. (2013) investigated the elastic and strength properties of mycelium biofoam in both tension and compression and found the strength of the biofoam decreases with increasing moisture content, and the compressive strength is almost three times the tensile strength. Travaglini et al. (2014) further investigated the flexural properties of mycology matrix core sandwich composites by four-point bend testing. In a recent article, Travaglini et al. (2015) tested the maximum use temperature, odor emission, and R -value of mycology materials and found they could be an attractive alternative to current insulation materials.

This study presents the bioengineering processes for the development of a white-rot fungal mycelium-based biofoam and characterization of its physical, thermal, and mechanical properties. Test results including dry density, thermal conductivity, Young's and shear moduli, stress-strain relationship, failure mode, and compressive strength are presented. The effectiveness of the processes and the impact of packing conditions and the addition of natural fiber are discussed.

Description of Bioengineering Process

Several mixing, packing, and incubating protocols have been explored to find the most promising bioengineering process. Table 1 specifies the groups according to the mixing, packing, and incubating protocols. Three batches of samples, designated as SP, SL, and SPL, respectively, were tested to evaluate the effectiveness of the incubation protocol and test status on the properties. The samples are right cylinders with a diameter of approximately 5 cm and a height of approximately 6 cm formed by polycarbonate tubular molds. The dried samples are slightly smaller than the mold dimensions because of shrinkage of biofoam in the drying process. Samples in SP and SL were incubated for 2 weeks, whereas

samples in SPL were the same as SL except that they were incubated for additional 4 weeks before testing. All samples except those in SL were dried in an oven set at 60°C for 24 h before testing. The only difference between SP and SL is that the samples in SP are dried, whereas samples in SL are live, and the difference between SP and SPL is the additional 4-week incubation applied to samples in SPL. Each batch had 30 samples, which were divided into six groups (G1–G6) to evaluate various blends of the biomass materials as a substrate and packing conditions for colonization of selected white-rot saprotrophic fungi cultures harvested from Alaska in molds. The blends comprised macerated sawdust pulp of Alaska birch (*Betula neoalaskana*) of 5 mm or smaller in size, millet grain, wheat bran, a natural fiber, and calcium sulfate.

In Mixing Protocol I, the feedstock ingredients (substrate) and live fungi culture were mixed and packed in molds, then placed in a temperature- and moisture-controlled incubator. In Mixing Protocol II, the substrate and the fungi culture were incubated in filtered polypropylene bags for a defined period before the blend was macerated and packed into the cylindrical molds, permitting it to reknit into a more structurally uniform and denser foam. Mixing Protocol III was the same as Protocol I but with natural fiber (50% of substrate's dry weight) added during mixing. Two packing conditions have been applied: loose and dense, the former being naturally deposited without compaction and the latter with approximately twice the original volume of materials packed. Fig. 1 illustrates the complete bioengineering process for Group 3 samples. Birch sawdust from the local forestry industry and added nutrients were mixed with a certain amount of water and pasteurized. Then,

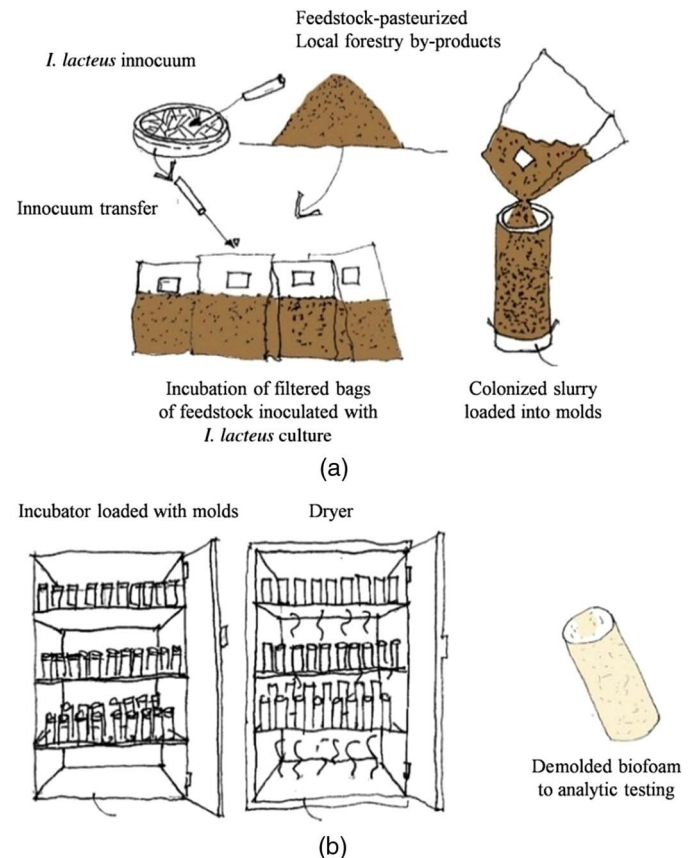


Table 1. Group Specification according to Mixing, Packing, and Incubating Protocols

Group number	Sample number	Mixing protocol	Packing	Incubation time/weeks	Test status
SP1	G1: SP01–SP05	I	Dense	Two	Dried
SP2	G2: SP06–SP10	I	Loose	Two	Dried
SP3	G3: SP11–SP15	II	Dense	Two	Dried
SP4	G4: SP16–SP20	II	Loose	Two	Dried
SP5	G5: SP21–SP25	III	Dense	Two	Dried
SP6	G6: SP26–SP30	III	Loose	Two	Dried
SL1	G1: SL01–SL05	I	Dense	Two	Live
SL2	G2: SL06–SL10	I	Loose	Two	Live
SL3	G3: SL11–SL15	II	Dense	Two	Live
SL4	G4: SL16–SL20	II	Loose	Two	Live
SL5	G5: SL21–SL25	III	Dense	Two	Live
SL6	G6: SL26–SL30	III	Loose	Two	Live
SPL1	G1: SPL01–SPL05	I	Dense	Six	Dried
SPL2	G2: SPL06–SPL10	I	Loose	Six	Dried
SPL3	G3: SPL11–SPL15	II	Dense	Six	Dried
SPL4	G4: SPL16–SPL20	II	Loose	Six	Dried
SPL5	G5: SPL21–SPL25	III	Dense	Six	Dried
SPL6	G6: SPL26–SPL30	III	Loose	Six	Dried

Fig. 1. Schematic of bioengineering sample preparing (images by Philippe Amstislavski): (a) prepare the raw samples; (b) dry and demold the samples

measure the P-wave velocity in the vertical (V_{VP}) and horizontal (V_{HP}) directions, respectively.

Wave Velocity Determination

Travel length and travel time need to be determined for evaluating wave velocity. The travel length is determined by measuring the tip-to-tip distance between the transmitter and receiver sensors. The time domain analysis method is used to determine the travel time. The P-wave first arrival is determined by the initial arrival of the transmitted P-wave because it is much faster than any S-waves in the system, as shown in Fig. 3. The determination of the S-wave first arrival is more difficult because of near-field effects, interference from faster P-waves in the system, and other factors. There are a number of ways to minimize the error involved in the S-wave first

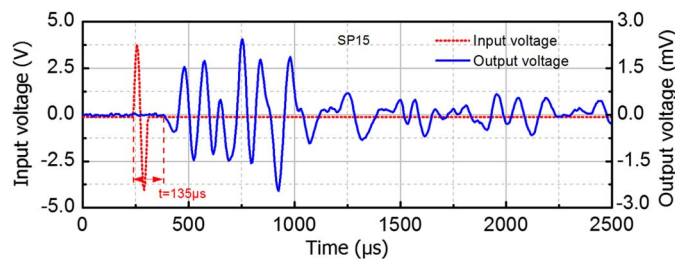


Fig. 3. Determination of P-wave first arrival for sample SP15 in vertical direction

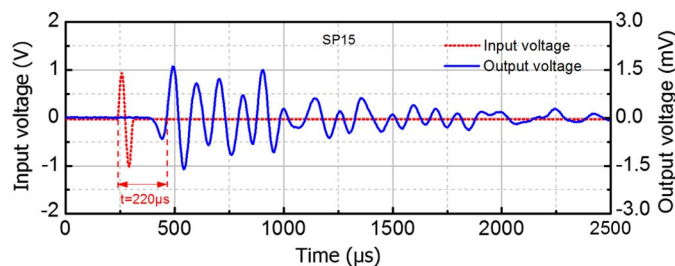


Fig. 4. Determination of S-wave first arrival for sample SP15 in vertical direction

arrival determination, and the zero after first bump method was used (Lee and Carlos Santamarina 2005), as illustrated in Fig. 4. However, the total travel time determined as illustrated is not the net travel time in the sample because there are system delays in the peripheral electronics, which can be measured by contacting the tips of the transmitting and receiving sensors. The system delay t_0 should be subtracted from the total travel time. The wave velocity is calculated using the following equation:

$$V = \frac{L}{\Delta t} = \frac{L}{t - t_0} \quad (4)$$

where V = wave velocity; L = travel distance; Δt = net travel time; t = total travel time; and t_0 = system delay.

Results and Analyses

This section presents and analyzes the results from various tests conducted for the three batches of samples. Only elastic moduli and thermal properties were measured for SL samples because this batch was later incubated for an additional 4 weeks (as identified as SPL) for further testing.

Sample Description and Failure Modes

Figs. 5(a–c) present images of three representative samples (e.g., SPL 12, SPL 17, and SPL 21) after the unconfined compression test to show the appearance of the biofoam and illustrate the failure modes of the biofoam under compression. SPL 12 was densely packed without natural fiber, SPL 21 was densely packed with natural fiber visible on the sample, and SPL 17 was loosely packed without natural fiber. One can observe from Fig. 5 that the biofoam samples have a chitinous skin formed around all the samples because of the polycarbonate molds, which constrained the mycelium growth in the radial direction and stimulated the generation of the outer skin when the expanding biomass of mycelium came in contact with the molds and formed a fairly strong protective layer on the circumferential surface of the sample. The skin was white when the sample was live and became off-white to beige when the sample was dried in the oven. Such a skin did not exist on the top and bottom surfaces of the samples because they were in contact with air during the incubating process. The substrate materials such as sawdust and natural fiber are still visible on the top

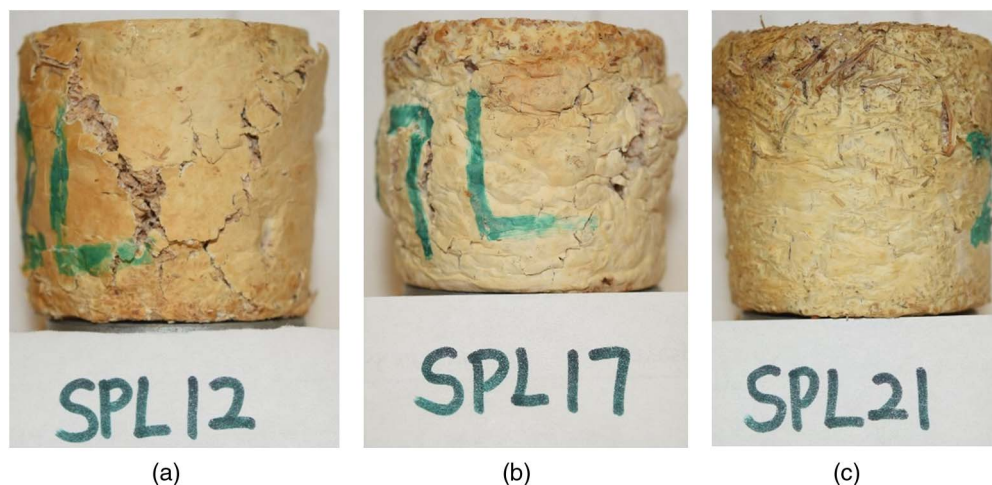


Fig. 5. Typical failure modes in the white-rot fungal mycelium-based biofoam under unconfined compression test: (a) shear failure; (b and c) bulging

and bottom of sample surfaces or when the material is cut or cracked.

In general, shear failure was observed for densely packed samples without natural fiber, as shown in Fig. 5(a) for SPL12, and bulging for loosely packed samples, as evidenced in Fig. 5(b) for SPL 17. When natural fibers were present, the samples all failed in bulging, regardless of the packing condition, as evidenced in Fig. 5(c) for SPL 21. The natural fiber prevented or minimized surface cracking on the samples during the unconfined compressive test. This is important because it would be more difficult for water to seep into the samples under loading. It is also visible from Fig. 5 that loosely packed samples (e.g., SPL 17) experienced substantially more plastic strain than densely packed samples after the compression test, given that the residual height for SPL 17 was noticeably shorter than the other two samples when their original height was approximately the same.

Elastic Moduli

The elastic moduli, including Young's and shear moduli, are basic stiffness properties for evaluating elastic deformation for engineering materials. Figs. 6 and 7 present the Young's and shear moduli in the vertical direction for SP, SL, and SPL batches of samples, respectively. In general, the Young's moduli for all groups of samples are much higher than the shear moduli. The packing condition has obvious impact on the stiffness, with the dense samples exhibiting higher stiffness than the loose samples given the same mixing protocol, and this impact can also be observed for other physical and mechanical properties presented throughout this study.

One can observe from Fig. 6 that the Young's modulus for SP samples in G3 and G4 is clearly larger than that for SPL samples, whereas the difference is not so obvious for other groups. The largest Young's modulus occurred for SP samples in G3 with a peak value of 60 MPa. The Young's moduli for SL batch samples are generally the smallest, with a peak value of 15 MPa occurring for G3 as well. Similar observations can be made for the shear modulus from Fig. 7. The largest shear modulus occurs in G3 of the SP batch, with a peak value of 24 MPa, and the smallest shear modulus also occurs in the SL batch. These results show that (1) both the Young's and shear moduli for G3 samples in the SPL batch are substantially smaller than those in the SP batch, (2) the elastic moduli of live samples are substantially smaller than

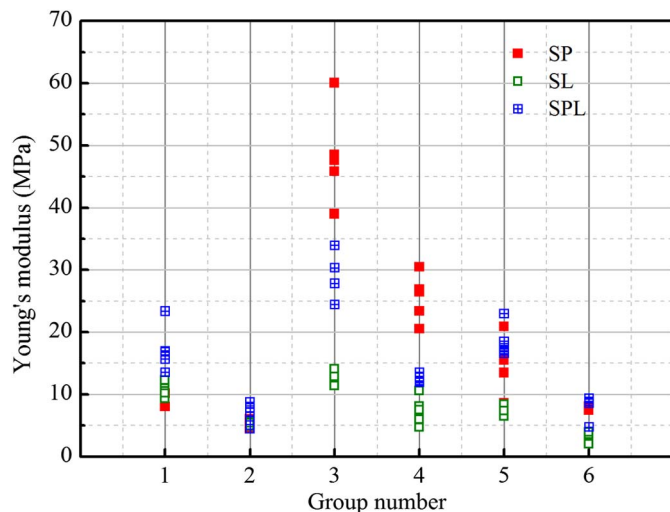


Fig. 6. Young's modulus of SP, SL, and SPL in vertical direction

those of dried samples with the same blend and packing conditions, and (3) an additional 4 weeks of incubation time has a mostly negative impact on Young's and shear moduli, particularly for G3 and G4 samples.

Anisotropy of Elastic Moduli

Anisotropy presents in most natural materials such as wood and soils. The elastic moduli in the horizontal direction were evaluated with the BE and PDE, methods as mentioned in the "Experimental Setup for Elastic Modulus Measurement" section, to examine whether anisotropy is present in biofoams. Figs. 8 and 9 present the elastic moduli in the horizontal direction in relation to those in the vertical direction for the SP and SPL samples, respectively. It is not surprising to observe anisotropy in elastic moduli from Figs. 9 and 10. It is, however, astonishing to find that the Young's and shear moduli in the horizontal direction for all samples in the SP and SPL batches are much higher than those in the vertical direction. The linear regression equations between the moduli in

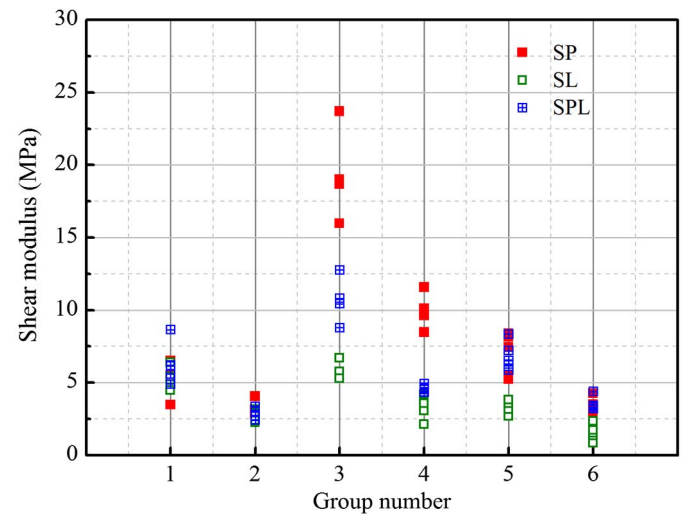


Fig. 7. Shear modulus of SP, SL, and SPL in vertical direction

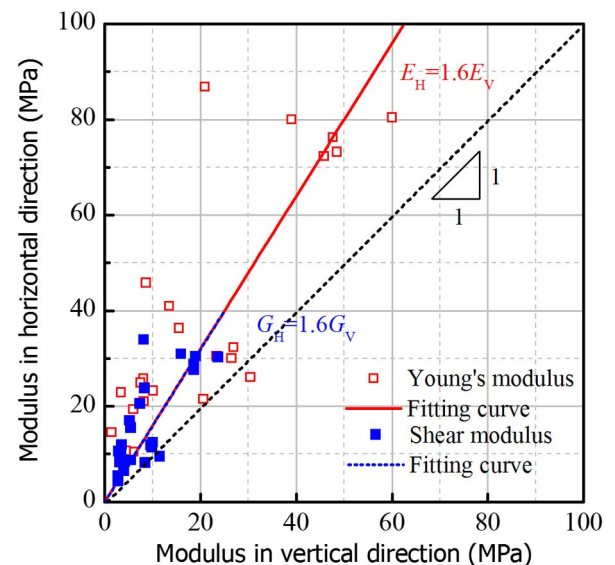


Fig. 8. Elastic modulus anisotropy of SP samples

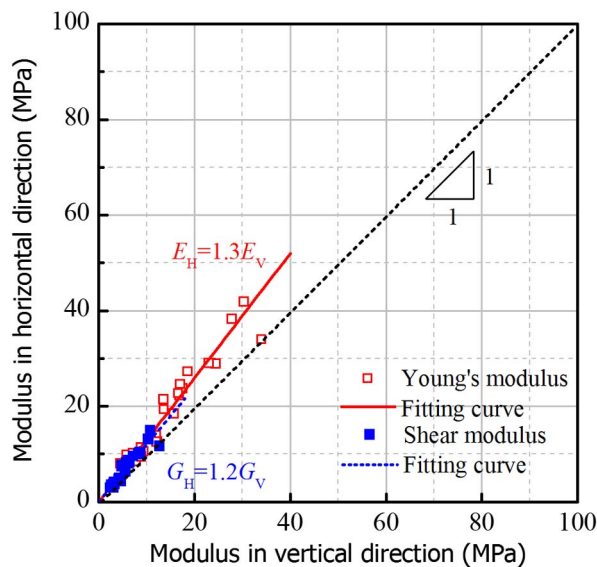


Fig. 9. Elastic modulus anisotropy of SPL samples

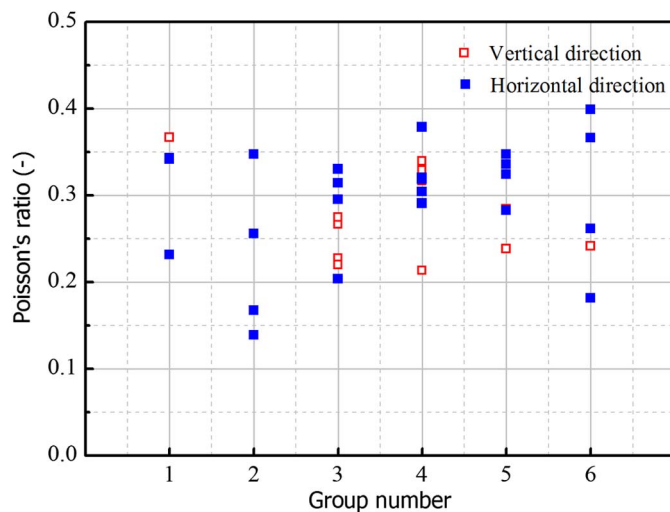


Fig. 10. Poisson's ratio of SP samples

the vertical and horizontal directions for the SP and SPL samples are presented in Figs. 8 and 9, respectively. Specifically, the Young's and shear moduli in the horizontal direction (E_H and G_H) are 60% larger than those in the vertical direction for the SP samples and 20–30% higher for the SPL samples. This strong elastic modulus anisotropy was likely induced by two mechanisms: the horizontal layers or fabric formed during packing of samples and the strong skin formed on the circumferential surface of the sample during incubation, as described in the "Sample Description and Failure Modes" section. The mycelium grows in random directions when the nutrients are uniformly distributed. The anisotropy of the SP samples was probably induced by the chosen packing method. As the mycelium keeps growing in the additional incubation period for the SPL samples, it digests the wood pulp, millet grain, and other nutrients, and gradually destroys the fabric or layering pattern formed during the packing process. However, because the samples are constrained by the cylindrical molds, the mycelium will not be able to grow randomly but vertically when it encounters the molds, therefore inducing a pattern in the internal

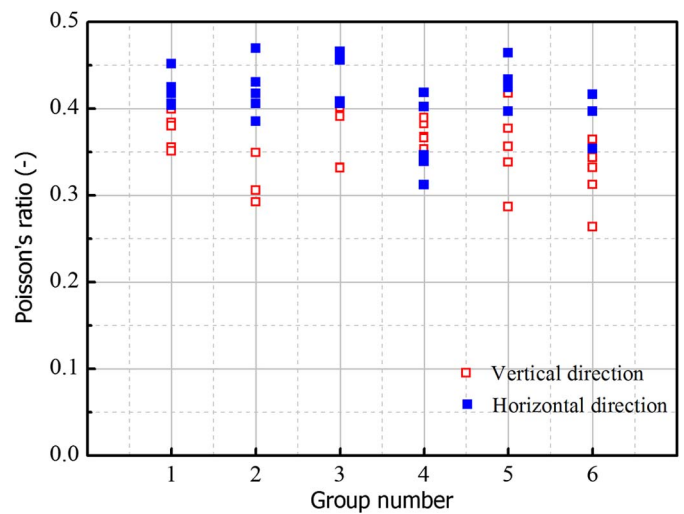


Fig. 11. Poisson's ratio of SPL samples

structure or anisotropy. The results indicate the anisotropy induced by both mechanisms is strong, with the packing method inducing even stronger anisotropy than the incubation method. Fig. 9 shows much less scattering than Fig. 8, implying that the anisotropy induced during the mycelium growth period is more consistent than that induced by packing.

Poisson's Ratio

The Poisson's ratios of the SP and SPL samples in the vertical and horizontal directions are computed using Eq. (3) based on the ratio of P-wave and S-wave velocity and presented in Figs. 10 and 11, respectively. One can observe from Fig. 10 that the Poisson's ratio for the SP samples varies between 0.15 and 0.45, as with many other foam materials. No clear separation can be observed between the Poisson's ratio in the vertical and horizontal directions. However, one can clearly see from Fig. 11 that the Poisson's ratio for the SPL samples varies between 0.25 and 0.5 with much less scattering due to more consistent anisotropy induced in the incubation process, and the Poisson's ratio in the horizontal direction is clearly larger than that in the vertical direction.

Stress-Strain Relationship and Compressive Strength

Samples in the same groups of SP and SPL batches exhibit similar stress-strain relationships in the unconfined compression test. For example, Fig. 12 shows stress-strain relationships for G1–G6 samples of the SPL batch. In general, like for soil materials, the stress-strain curve exhibits strain-softening behavior for densely packed samples such as SPL02 and SPL12, and strain-hardening behavior for loosely packed samples such as SPL08 and SPL17. For the samples with natural fiber included in the substrate such as SPL 21 and SPL26, the stress-strain relationships exhibit strain-hardening behavior regardless of the packing condition because the natural fiber serves to reinforce the biofoam and prevent shear failure.

The compressive strength can be obtained from the stress-strain relationships for each sample. It is defined as the peak stress when a peak occurs in the stress-strain relationship (strain-softening behavior) or the stress at 15% strain when no peak occurs in the stress-strain relationship (strain-hardening behavior). Fig. 13 presents the compressive strength of the SP and SPL samples. The compressive strengths for G3 samples are substantially larger

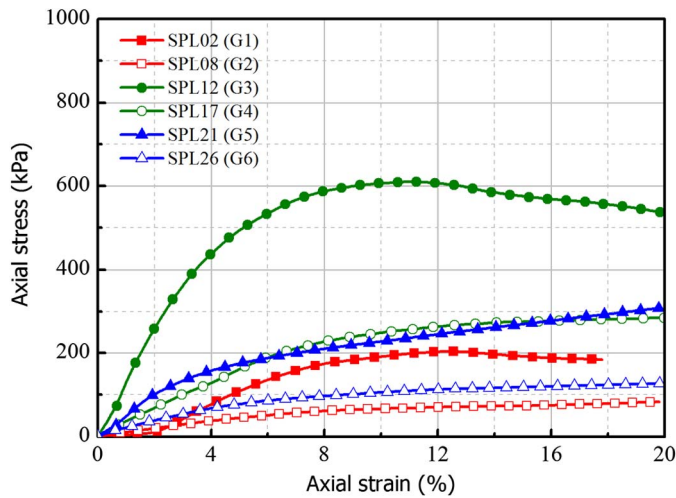


Fig. 12. Typical stress-strain relationships in unconfined compression test

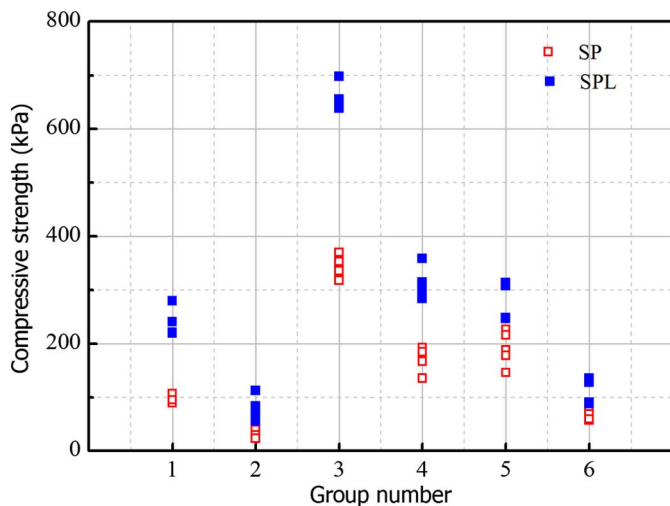


Fig. 13. Compressive strength of SP and SPL samples

than other groups in both the SP and SPL batches. One can also observe a substantial increase in the compressive strength when the incubation time increases from 2 to 6 weeks, especially for G3 samples.

Thermal Conductivity

Fig. 14 presents the thermal conductivity of the SP, SL, and SPL samples. The thermal conductivity values of live samples (SL samples) are in the range of 0.13–0.40 W/(m · K), and those of dried samples (SP and SPL samples) fall into a much smaller range, i.e., 0.05–0.07 W/(m · K). The larger values and more scattering in thermal conductivity of live samples are due to high moisture content and varying packing conditions of the different blends. The variation of thermal conductivity is still visible, but much smaller for dried samples. This substantial drop in thermal conductivity for dried samples is expected and is because the varying amount of moisture existing in the substrates and mycelium of live samples is replaced with low-thermal-conductivity air during the drying process.

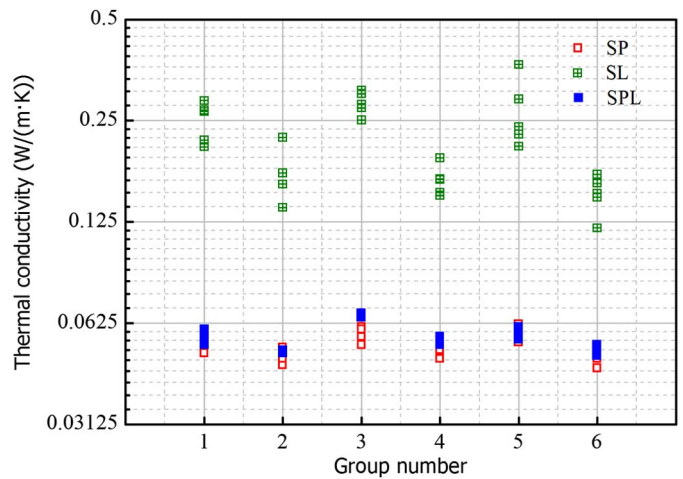


Fig. 14. Thermal conductivity of SP, SL, and SPL samples

Discussion

To allow further examination of the characteristics of different groups of blends, the physical, thermal, and mechanical properties such as dry density, Young's and shear moduli, compressive strength, and thermal conductivity of samples in each group were averaged and are presented in Fig. 15. Higher values for Young's and shear moduli suggest less elastic deformation and better handling performance during installation, whereas higher compressive strength suggests less chance of damage when a large load is applied. Lower thermal conductivity is desirable for thermal insulation materials. Fig. 15 shows that the average dry density of densely packed samples is in a range of 240–265 kg/m³ for SP samples and 230–280 kg/m³ for SPL samples. The average dry density of loosely packed samples is in a range of 165–195 kg/m³ for SP samples and 160–280 kg/m³ for SPL samples. The dry density of loosely packed samples with natural fiber is considerably lower than those without natural fiber. The impact of additional incubation time on density is mixed, with a slight increase observed for G2, G5, and G6 samples and a slight decrease observed for G3 samples. Overall, this biofoam is much lighter than water, soils, or most other materials used in the civil engineering industry.

One can observe from Fig. 15 that the thermal conductivity of the SPL samples is only slightly larger than the SP samples, even if the SPL samples were incubated for an additional 4 weeks. It is quite clear that the additional incubation time substantially decreases the Young's and shear moduli for the G3 and G4 samples, which have relatively higher moduli. The average Young's modulus of the G3 samples decreases from 50 to 30 MPa, and the shear modulus decreases from 19 to 11 MPa, or by approximately 40%. The decrease is very likely due to further fungal digestion of granular substrates such as millet grain and calcium sulfate, which otherwise contributed to the elastic stiffness in the earlier stage of mycelium growth. However, the compressive strength for all groups sees noticeable gains with increasing incubation time, with the largest absolute value increase occurring for G3 samples, from 350 to 570 kPa, or over 60%. The increase can probably be attributed to the growth of mycelium that serves as a random matrix binding together the substrate. In summary, densely packed samples following Mixing Protocol II have the highest dry density, Young's and shear moduli, compressive strength, and comparable thermal conductivity among all sample groups.

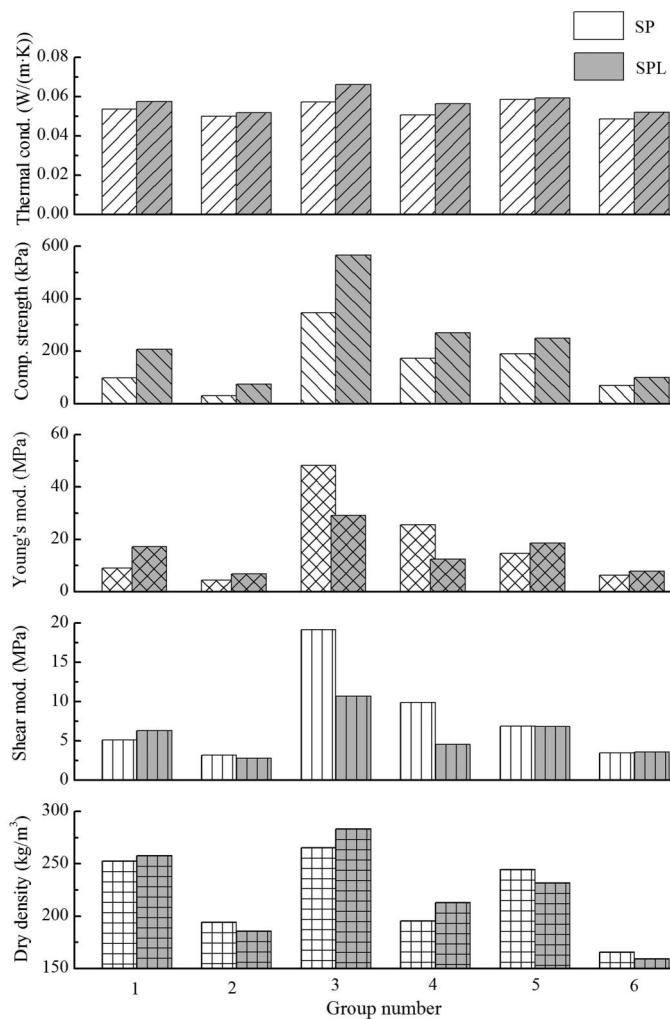


Fig. 15. Physical, thermal, and mechanical properties of mycelium-based biofoam

As mentioned before, Mixing Protocol III (i.e., samples in G5 and G6) is the same as Mixing Protocol I (i.e., samples in G1 and G2) but with natural fiber added. Comparing the properties of G1 with G5, or G2 with G6 of the same packing condition in either the SP or SPL batch, it is interesting to observe that the addition of natural fiber consistently increased the Young's and shear moduli and compressive strength, even when the addition of natural fiber decreased the dry density. The natural fiber plays a positive role in the mycelium-based biofoam overall structure because it helps increase the elastic stiffness, changes the failure mode from potential shear failure to bulging for dense samples, and prevents or reduces occurrence of surface cracks.

Development of this biofoam is still in its early stage. However, the potential of such a biofoam can perhaps be demonstrated by comparing its properties with Insulfoam (ARCAT, Inc. 2012), an expanded polystyrene foam widely used as insulation material in the building and infrastructure construction industry, particularly in cold regions. The density of Insulfoam is in the range of 16–48 kg/m³, the thermal conductivity in the range of 0.03–0.04 W/(m · K), and the compressive strength in the range of 69–400 kPa. The compressive strength of mycelium-based biofoam meets or exceeds that of Insulfoam products, and the thermal conductivity is slightly higher. The density is considerably

higher than Insulfoam and could be improved for practical applications.

Conclusions

This paper presents an innovative fungal mycelium-based biofoam. Three different mixing protocols with various substrate materials, including wood pulp, millet grain, wheat bran, natural fiber, and calcium sulfate, and two packing conditions were tested to produce three batches of samples for physical, thermal, and mechanical property characterization. Dry density, thermal conductivity, elastic moduli including Young's and shear moduli, Poisson's ratio, and compressive strength were obtained. Based on the findings from this study, the following conclusions can be drawn:

1. This biofoam is relatively lighter weight than water, soils, or most other materials used in the civil engineering industry;
2. Results show that densely packed samples following Mixing Protocol II, i.e., G3 samples, have the highest dry density, elastic moduli, and compressive strength;
3. The dried biofoam demonstrates good thermal conductivity, which falls in the range of 0.05–0.07 W/(m · K). Live samples possess higher conductivity because of the existence of relatively high moisture content;
4. This biofoam exhibits fairly good elastic moduli when it is dried. However, the live sample exhibits much lower elastic moduli;
5. This biofoam exhibits strong elastic anisotropy, with Young's and shear moduli in the horizontal direction 20–60% larger than those in the vertical direction. This strong elastic anisotropy can be attributed to the packing method and a strong skin formed on the circumferential surface of samples during the incubation process;
6. This biofoam demonstrates excellent compressive strength, with an average value of 350–570 kPa for G3 samples;
7. The incubation time has a small impact on the dry density and thermal conductivity, a negative impact on the elastic moduli, but a clear positive impact on the compressive strength;
8. The addition of natural fiber helps improve the elastic moduli and compressive strength, changes the failure mode of densely packed samples from shear failure to bulging, and prevents or minimizes the occurrence of surface cracks during compression tests; and
9. This biofoam has met or exceeded like characteristics of the conventional polymeric thermal foams except dry density.

Future study of such a biofoam should focus on fire resistance, water absorption issues, and the impact of environmental conditions. This study, however, demonstrates that this fungal mycelium-based biofoam offers great potential for application as an alternative insulation material for building and infrastructure construction, particularly in cold regions, or an alternative light-weight backfill material for geoenvironmental engineering.

Acknowledgments

The authors gratefully appreciate the financial support provided by the Innovate Award from the University of Alaska Anchorage, Anchorage, United States. The authors are especially thankful to Dr. Helena S. Wisniewski for her encouragement and support for this study. Last, but not least, the authors express appreciation to the following individuals for their contributions to this project: Dr. Fred Rainey, Dr. Bjartmar Sveinbjörnsson, John Moore, Tim Kirk, and Dasha Petrov.

References

- Arifin, Y. H., and Yusuf, Y. (2013). "Mycelium fibers as new resource for environmental sustainability." *Proc. Eng.*, 53, 504–508.
- ASTM. (2013). "Standard test method for unconfined compressive strength of cohesive soil." *ASTM D2166-13*, West Conshohocken, PA.
- ASTM. (2014). "Standard test method for determination of thermal conductivity of soil and soft rock by thermal needle probe procedure." *ASTM D5334-14*, West Conshohocken, PA.
- Bandyopadhyay, A., and Basak, G. C. (2007). "Studies on photocatalytic degradation of polystyrene." *Mater. Sci. Technol.*, 23(3), 307–314.
- De Alba, P., Baldwin, P. K., Janoo, V., Roe, G., and Celikkol, B. (1984). "Elastic-wave velocities and liquefaction potential." *Geotech. Test. J.*, 7(2), 77–88.
- Decagon Devices, Inc. (2015). "Operator's manual for KD2 pro thermal properties analyzer." Pullman, WA.
- Dicker, M. P. M., Duckworth, P. F., Baker, A. B., Francois, G., Hazzard, M. K., and Weaver, P. M. (2014). "Green composites: A review of material attributes and complementary applications." *Compos.: Part A: Appl. Sci. Manuf.*, 56, 280–289.
- Dyvik, R., and Madshus, C. (1985). "Lab measurements of Gmax using bender element." *Proc., ASCE Convention on Advances in the Art of Testing Soils under Cyclic Conditions*, ASCE, Reston, VA, 186–196.
- Eben, B., and Gavin, M. (2011). "Method for producing rapidly renewable chitinous material using fungal fruiting bodies and product made thereby." United States Patent and Trademark Office, Alexandria, VA.
- Eseller-Bayat, E., Gokyer, S., Yegian, M. K., Deniz, R. O., and Alshawabkeh, A. (2013). "Bender elements and bending disks for measurement of shear and compression wave velocities in large fully and partially saturated sand specimens." *Geotech. Test. J.*, 36(2), 1–8.
- Gurunathan, T., Mohanty, S., and Nayak, S. K. (2015). "A review of the recent developments in biocomposites based on natural fibres and their application perspectives." *Compos.: Part A: Appl. Sci. Manuf.*, 77, 1–25.
- Hofer, T. N. (2008). "Marine pollution: New research." Nova Science Publishers, New York, 59.
- Holt, G. A., McIntyre, G., Glagg, D., Wanjura, J. D., and Pelletier, M. G. (2012). "Fungal mycelium and cotton plant materials in the manufacture of biodegradable molded packaging material: Evaluation study of select blends of cotton byproducts." *J. Biobased Mater. Bioenergy*, 6(4), 431–439.
- Insulfoam. (2014). "Carlisle Company: Insulation and roofing." (<http://www.arcacat.com/arcacatcos/cos0434/arc34935.html>) (Jul. 7, 2015).
- Lee, J. S., and Carlos Santamarina, J. (2005). "Bender elements: Performance and signal interpretation." *J. Geotech. Geoenviron. Eng.*, 10.1061/(ASCE)1090-0241(2005)131:9(1063), 1063–1070.
- Leong, E. C., Yeo, S. H., and Rahardjo, H. (2005). "Measuring shear wave velocity using bender elements." *Geotech. Test. J.*, 28(5), 1–11.
- Moriana, R., Vilaplana, F., Karlsson, S., and Ribes-Greus, A. (2011). "Improved thermo-mechanical properties by the addition of natural fibres in starch-based sustainable biocomposites." *Compos. Part A: Appl. Sci. Manuf.*, 42(1), 30–40.
- Morreale, M., Scaffaro, R., Maio, A., and La Mantia, F. P. (2008). "Effect of adding wood flour to the physical properties of a biodegradable polymer." *Compos. Part A: Appl. Sci. Manuf.*, 39(3), 503–513.
- Padula, V. M., Stewart, S., and Causey, D. (2014). "The impacts of plastic on western Aleutian Islands seabirds: Detection of phthalates in muscle and embryonic tissues." *Proc., 16th Alaska Bird Conf.*, Juneau, AK.
- Paul, V., Kanny, K., and Redhi, G. G. (2015). "Mechanical, thermal and morphological properties of a bio-based composite derived from banana plant source." *Compos.: Part A: Appl. Sci. Manuf.*, 68, 90–100.
- Pelletier, M. G., Holt, G. A., Wanjura, J. D., Bayer, E., and McIntyre, G. (2013). "An evaluation study of mycelium based acoustic absorbers grown on agricultural by-product substrates." *Ind. Crops Prod.*, 51, 480–485.
- Shirley, D. J., and Anderson, A. L. (1975). "Acoustic and engineering properties of sediments." *Rep. ARL-TR-75-58*, Applied Research Laboratory, Univ. of Texas, Austin, TX.
- Travaglini, S., Dharan, C., and Ross, P. G. (2014). "Mycology matrix sandwich composites flexural characterization." *Proc., 29th Technical Conf. of the American Society for Composites*, H. Kim, D. Whisler, and Z. M. Chen, et al., eds., DEStech Publications, Inc., Lancaster, PA, 1–20.
- Travaglini, S., Dharan, C. K. H., and Ross, P. G. (2015). "Thermal properties of mycology materials." *Proc., 30th Technical Conf. of the American Society for Composites*, X. Xiao, A. Loos, and D. Liu, eds., DEStech Publications, Lancaster, PA, 1–17.
- Travaglini, S., Noble, J., Ross, P. G., and Dharan, C. K. H. (2013). "Mycology matrix composites." *Proc., 28th Annual Technical Conf. of the American Society for Composites*, C. Bakis, ed., DEStech Publications, Inc., Lancaster, PA, 517–535.